Semiconductor Optical Amplifier-Assisted Optical Wireless Links: The Effect of Noise and Turbulence

Konstantinos Yiannopoulos*, Nikos C. Sagias*, and Anthony C. Boucouvalas*
*Department of Informatics & Telecommunications, University of Peloponnese, Akadimaikou G. K. Vlahou street, 22100 Tripoli, Greece
(nsagias@ieee.org, kyianno@uop.gr, acb@uop.gr)

***Abstract*—We present an analytical framework for estimating the benefits that arise from the utilization of semiconductor optical amplifiers (SOA)s at fade impaired outdoor optical wireless systems. We first investigate the impact of fading on both the signal optical power and the amplified spontaneous emission, and derive analytical relations that accurately associate the system bit-error-rate (BER) with the channel state. We then utilize the analytical relations to assess the performance of the amplified optical signal under moderate-to-strong fading and demonstrate that the sensitivity improvement, which is expected by the amplification process, improves the first- and second-order signal-to-noise ratio statistics at the electronic receiver. Our results show that the average BER and average fade duration can all be drastically reduced by the incorporation of the SOA, provided that the link length remains within reasonable limits that are dictated by the channel statistics.**

***Index Terms*—Bit-error-rate (BER), level crossing rate (LCR), average fade duration (AFD), gamma-gamma fading, outdoor optical wireless, semiconductor optical amplifier (SOA).**

I. Introduction

Optical wireless communications (OWC) have drawn considerable attention as a means of implementing reliable high-capacity outdoor systems that may not be implemented by conventional fiber optics [1]. Hero experiments involve intersatellite or satellites-to-earth links that have demonstrated the potential of OWC system utilization in extreme application scenarios [2], culminating in the recent moon-to-earth communication [3]. Outdoor OWC are equally important in down-to-earth systems that are used to interconnect buildings or business networks in urban environments at very high capacities that are comparable with fiber-based solutions [4]. The widespread application of outdoor OWC, however, is hindered by atmospheric effects that induce a severe penalty on the link budget. Fog, snow, rain and air pollution account for a relatively static loss in the OWC channel that needs to be compensated by amplification, coding and/or diversity [5], [6], while the existence of variable temperature air pockets in the transmission path imparts a time-varying loss that is generally described as fading. Fading is typically tackled by providing an adequate link margin, while a number of techniques have been proposed with a goal of reducing the impact of fading and minimizing the margin that is required. Beam focusing [7], aperture averaging [8]–[10], spatial and temporal diversity [10]–[12], coding [13], [14], relaying [15]–[18] and amplification [16], [19] are candidate techniques that have been proposed to effectively minimize the impact of fading and contribute to more reliable outdoor OWC links.

Within the context of fade mitigation, we recently studied the performance of a semiconductor optical amplifier (SOA) assisted OWC system in the presence of moderate-to-strong fading [20]. Based on a technique that was experimentally investigated earlier [19], we provided an analytical framework for assessing key metrics of the SOA-assisted system operation, including the outage probability and average fade duration, and demonstrated that the SOA can provide a very significant level of 2R regeneration. We also concluded, however, that optimal regeneration requires optical powers of the same order of magnitude with the SOA saturation power (a few dBm). Even though this could be the case in a relay, which will restore and retransmit the OWC signal, typical optical receivers exhibit sensitivities of approximately 30 dB lower than the SOA saturation power, and the proposed technique does not provide a regenerative benefit at the link endpoint.

While relaying techniques aim to periodically regenerate the optical signal along the transmission path, and thus result in a more reliable OWC system, optical amplification at the receiver achieves enhanced reliability by improving the receiver sensitivity rather than the quality of the optical signal [21], [22]. The improved receiver sensitivity adds to the link margin and as a result more intense fading can be tolerated at the OWC link. To our knowledge, a full analysis of the beneficial impact of the sensitivity improvement due to amplification has only been performed for first-order statistics in the weak (log-normal) turbulence regime [23], while no related work has been recorded for moderate-to-strong (γ–γ) turbulence or second-order statistics. In this work, we assess the beneficial impact of the SOA on the receiver performance by analytically associating the optical noise components that arise from the amplification process with the γ–γ channel state. This approach enables the accurate calculation of the electrical noise variances, and consequently the system bit-error-rate (BER), for any given channel state; as a result, key first- and second-order metrics can be calculated in a straightforward fashion by treating the BER as a random variable (rv) that directly correlates with the γ–γ channel [24].

The rest of this paper is organized as follows: In Section II we present the mathematical model that describes the BER performance of the system in the presence of γ–γ fading. The mathematical model makes no assumptions on the signal and noise contributions, both electrical and optical, that affect the system so as to accurately calculate its performance. In Section III we analytically evaluate the SOA-assisted system performance in terms of average BER. The evaluation is carried out for both channel state aware (optimum) and non-aware (sub-optimum) receivers, after further optimizing their performance by taking into account the impact of channel

fading on the instantaneous system BER. Section IV discusses the second-order statistics performance of the system and its main contribution is the analytical derivation of the level crossing rate (LCR) and the average fade duration (AFD) at the presence of the SOA. Our results show that the expected duration of fades is decreased by at least 75% of its original value without the SOA, thus verifying the superior performance of the SOA-assisted system. We also demonstrate in this section that the second-order statistics can be calculated in a straightforward fashion from the improved sensitivity, which makes this work readily applicable to all turbulence regimes irrespective of their strength. Finally, Section V discusses future studies and concludes the paper.

II. Preliminaries, Turbulence and Noise Model

As it has been extensively described [20], the SOA-based fade mitigation technique utilizes a SOA to partially alleviate the impact of fades on the OWC signal. Following the analysis found therein, the transmitted optical signal experiences time-varying power fluctuations due to fading, and these fluctuations occur at timescales significantly greater than the bit period. This corresponds to a slow modulation of the amplitude of thousands of successive optical pulses, which gradually diminish in power while the channel enters a fade state. Due to the slow modulation process the pulses profiles are not distorted and each pulse can be in principle restored independently by signal processing regeneration techniques, including SOA-based 2R regenerators.

Even though signal restoration is particularly appealing, especially in intermediate relays, a more typical role for SOAs in OWC systems would be to simply provide a static gain that compensates for link losses or provides the required fade margin. An interesting and potentially useful aspect of utilizing the SOA in this fashion stems from the observation that the amplifier modifies the noise properties of the system and a dominant electrical noise component emerges from the beating between the optical signal and the amplified spontaneous emission on the receiver photodiode. This leads to an extended sensitivity improvement at the receiver that adds to the available link budget, providing a direct benefit from using the amplifier. An in-depth treatment of the amplified system, however, requires the development of an analytical model that takes into account the impact of fading both on the signal power and the electrical noise variances. This association enables the calculation of the system BER in any given channel state and its treatment as a rv, which also allows the derivation of first- and second-order statistics for the optical signal in terms of the BER rather than absolute or normalized power levels.

The main goal of this section is to derive analytical equations for the amplified system BER as a rv whose value is determined by the channel state. We assume that the OWC system utilizes return-to-zero (RZ) on/off optical pulses, which experience slowly varying power fluctuations, due to fading, and that the optical power $P_{\rm in}$ of each received pulse at the input of SOA is a rv, following the preceding discussion. In the context of the current work $P_{\rm in}$ obeys γ–γ statistics with a probability density function (pdf)

$$f_{P_{\rm in}}(z) = \frac{2\,(m_y\,m_x)^{\frac{m_y+m_x}{2}}}{\Gamma(m_x)\,\Gamma(m_y)}\,\frac{z^{\frac{m_y+m_x}{2}-1}}{\overline{P}_{\rm in}^{\frac{m_y+m_x}{2}}} \times K_{m_y-m_x}\left(2\sqrt{m_y\,m_x\,\frac{z}{\overline{P}_{\rm in}}}\right), \tag{1}$$

where $\overline{P}_{\rm in}$ is the average SOA input optical power, while $\Gamma(\cdot)$ and $K_v(\cdot)$ denote the Gamma and second-kind modified Bessel functions, respectively [25]. Moreover, m_x and m_y are two γ–γ distribution parameters related to the effective numbers of large- and small-scale scatterers in the OWC link.

The optical pulses traverse the SOA and, depending on the channel state, partially saturate it. For a the RZ line coded system, the power transfer function that relates the output and input powers per optical pulse is given by [26]

$$P_{\rm out}(z) = P_{\rm sat}\,\log_{10}\left[1+G\left(\exp\left(\frac{z}{P_{\rm sat}}\right)-1\right)\right], \tag{2}$$

where G is the SOA small-signal gain, $P_{\rm sat}$ is the rate-dependent saturation parameter of the SOA

$$P_{\rm sat} = \frac{U_{\rm sat}}{T_b}, \tag{3}$$

$U_{\rm sat}$ is the SOA saturation energy and T_b is the bit duration. Nonlinear gain saturation effects are included in this work primarily for model consistency purposes and do not affect the OWC system operation or the attained results to any significant degree. In practice, the received power levels of practical OWC systems are not sufficient to saturate the SOA gain, especially in the presence of fading, and the device exhibits almost linear gain. Apart from providing a certain degree of gain to the incoming signal, the SOA also generates a significant amplified-spontaneous-emission (ASE) optical noise component with a power density

$$P_n = n_{sp}\,h\,\frac{c}{\lambda}. \tag{4}$$

In the last equation, c is the vacuum light speed, h is the Planck constant, n_{sp} is the population inversion factor and λ denotes the wavelength. The ASE noise beats with the received signal on the receiver photo-diode, and a number of electrical noise components manifest at the input of the electronic receiver. The noise components are described by the following noise variances that mathematically describe the thermal σ^2_{th}, shot σ^2_{shot}, signal-spontaneous beating σ^2_{sig-sp} and spontaneous-spontaneous beating σ^2_{sp-sp} contributions as

$$\sigma^2_{th} = \frac{4\,k_B\,T\,F_n\,B_e}{R_L}, \tag{5a}$$

$$\sigma^2_{shot}(z) = 2\,q\,R\,\left(P_{\rm out}(z) + (G-1)\,P_n\,B_o\right)\,B_e, \tag{5b}$$

$$\sigma^2_{sig-sp}(z) = 4\,R^2\,P_{\rm out}(z)\,(G-1)\,P_n\,B_e, \tag{5c}$$

and

$$\sigma^2_{sp-sp} = 2\,R^2\,\left((G-1)\,P_n\right)^2\,(2\,B_o - B_e)\,B_e, \tag{5d}$$

TABLE I
OWC SYSTEM PARAMETERS

Parameter	Symbol	Value
Refractive index structure	C_n^2	4.58×10^{-13} m$^{-2/3}$
Receiver aperture diameter	D	10 mm
Link length	L	250, 500, 1000 m
Wavelength	λ	1550 nm
Line Rate	${T_b}^{-1}$	10 Gb/s
SOA small-signal gain	G	20 or 30 dB
Saturation parameter	P_{sat}	1 mW
Population inversion factor	n_{sp}	4.0
Photodiode responsivity	R	1.25 A/W
Receiver temperature	T	300^o K
Resistor load	R_L	$100\,\Omega$
Electrical noise figure	F_n	3 dB
Electrical bandwidth	B_e	7 GHz
Optical bandwidth	B_o	50 GHz

TABLE II
GAMMA-GAMMA CHANNEL PARAMETERS

L (m)	m_x	m_y	$\sigma_{\gamma-\gamma}$	b_x	b_y
250	5.93	1.99	0.87	18.19	30.14
500	4.20	0.83	1.31	11.56	42.83
1000	5.54	0.39	1.79	3.93	48.46

respectively [21]. In (5), B_e and B_o are the electrical and optical bandwidths, respectively, R is the photodiode responsivity, T is the receiver temperature, k_B denotes the Boltzmann constant, F_n is the electric noise figure and R_L is the resistor load. All these parameters are summarized in Table I. In all the above expressions, the SOA small signal gain is used to calculate the noise variances despite the fact that the gain is compressed due to saturation effects, as it is clearly predicted by (2). It is noted here that this approximation does not affect the key contributions of this work. In fact, the noise powers, that are predicted by (5), are higher than those that would be calculated after taking into consideration the gain saturation and, as a result, this work can serve as the *worst-case scenario*.

III. AVERAGE BIT-ERROR-RATE ANALYSIS

In the current section we discuss the improvement that is achieved by introducing the SOA at the OWC system receiver in terms of first-order statistics. By utilizing the mathematical framework that we developed in the previous section, we assess the average BER of a SOA-assisted system and demonstrate that the SOA provides a link margin that can fully compensate for any practically considered fade margin.

Given (2) and (5), it is possible to estimate the signal and noise electrical powers when the on '1' and off '0' symbols are transmitted on the optical link as

$$I_1(z) = R\,P_{\rm out}(z)\,, \tag{6a}$$

$$\sigma_1^2(z) = \sigma_{th}^2 + \sigma_{shot}^2(z) + \sigma_{sig-sp}^2(z) + \sigma_{sp-sp}^2\,, \tag{6b}$$

and

$$I_0 = 0\,, \tag{7a}$$

$$\sigma_0^2 = \sigma_{th}^2 + \sigma_{shot}^2(0) + \sigma_{sp-sp}^2\,, \tag{7b}$$

respectively. Then, the BER performance of the system is evaluated by

$$BER(z) = \frac{1}{4}\,\mathrm{erfc}\left(\frac{I_1(z)-I_{th}}{\sigma_1(z)\sqrt{2}}\right) + \frac{1}{4}\,\mathrm{erfc}\left(\frac{I_{th}}{\sigma_0\sqrt{2}}\right)\,, \tag{8}$$

where I_{th} is the decision threshold of the electronic receiver, and the average BER can be calculated from (8) after integrating over all possible channel states to obtain

$$\overline{BER} = \int_0^\infty BER(z)\,f_{P_{\rm in}}(z)\,dz\,. \tag{9}$$

One key challenge here is to determine the decision threshold I_{th} at the receiver so as to achieve optimal average BER performance. We will investigate the system operation assuming that the receiver is both non-aware and aware of the channel state:

A. Reception without CSI

If the receiver can not acquire information about the channel state (non-CSI receiver) and the decision threshold has to be a-priori set during the link establishment, then optimal operation is achieved for a maximum-likelihood threshold that is calculated after differentiating (9) with respect to I_{th} to finally obtain

$$\int_0^\infty \frac{\exp\left(-\frac{(I_1(z)-I_{th})^2}{2\sigma_1^2(z)}\right)}{\sigma_1(z)}\,f_{P_{\rm in}}(z)\,dz \;=\; \frac{\exp\left(-\frac{I_{th}^2}{2\sigma_0^2}\right)}{\sigma_0}\,. \tag{10}$$

B. Reception with CSI

If the receiver is capable of monitoring the channel state, then a symbol-by-symbol decision threshold can set for each respective channel state. In this case the threshold for any given state can be approximated by [27]

$$I_{th}(z) = \frac{\sigma_0\,I_1(z)}{\sigma_0+\sigma_1(z)}\,, \tag{11}$$

and (9) simplifies to

$$\overline{BER} = \frac{1}{2}\int_0^\infty \mathrm{erfc}\left(\frac{Q(z)}{\sqrt{2}}\right)\,f_{P_{\rm in}}(z)\,dz\,, \tag{12}$$

with

$$Q(z) = \frac{I_1(z)}{\sigma_0+\sigma_1(z)}\,. \tag{13}$$

Eqs. (9) and (12) are plotted against the average received optical power $\overline{P}_{\rm in}$ in Figs. 1 and 2 for two SOAs with small signal gains of 20 and 30 dB, and three OWC links with distances of 250, 500 and 1000 m. The parameters that were used to obtain the graphs are summarized in Tables I and II and correspond to a sensitivity improvement of 14.3 dB for a BER target of 10^{-3} and 12.5-13.8 dB for a BER target of 10^{-6}, depending on the SOA gain.

The results demonstrate a 17 dB power margin improvement when the SOA is deployed in the non-CSI system irrespective of the link length. The margin improvement is decreased by

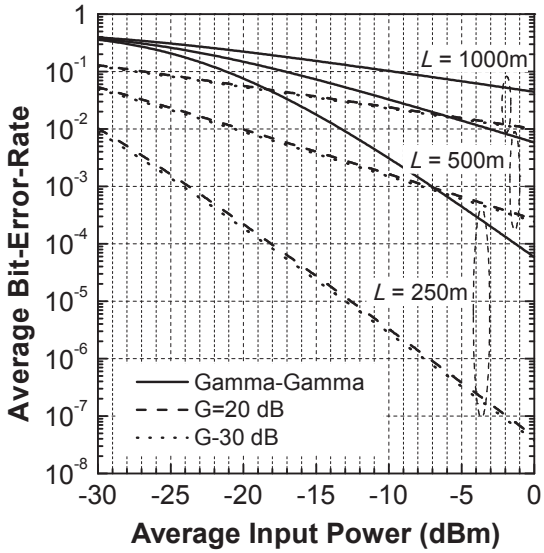

Fig. 1. Average bit-error-rate versus the average input power for a non-CSI receiver. The original non-amplified (γ–γ) system is also shown for reference.

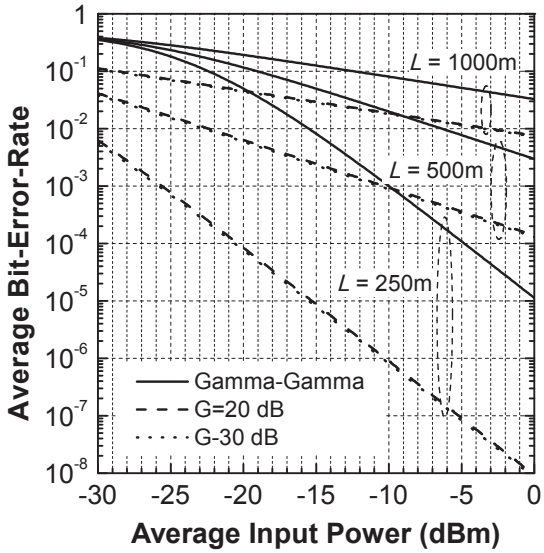

Fig. 2. Average bit-error-rate versus the average input power for a CSI receiver. The original non-amplified (γ–γ) system is also shown for reference.

approximately 1 dB in the CSI system, since the receiver is partially capable of self-adjusting to link fades. Clearly, the SOA plays the most important role in fade mitigation, providing a significant benefit on the link budget, and will either (*a*) allow for higher link availability whenever the rest of the static (rain/snow/fog) and time varying losses (building sway) are accounted for, as we demonstrate in the next section, or (*b*) allow for the power budget re-distribution to compensate for effects other than fading in systems that are transmission power limited, for example due to eye-safety considerations.

IV. Second-Order Statistics Analysis

The goal of this section is to evaluate the performance of the SOA-assisted system in terms of the second-order statistics and mainly the level crossing rate and the average fade duration. In contrast with existing works that discuss the second-order properties of the system in terms of power thresholds, we focus on the actual BER properties of the SOA-assisted system and derive the LCR and AFD for a target BER level BER_0. To this end, we first evaluate the system LCR and then utilize the AFD definition to obtain analytical results.

The LCR is calculated from the joint pdf of the optical signal power z and its time derivative $\dot{z}$. For a $\gamma-\gamma$ channel the joint pdf is given by [28]

$$f_{v,\dot{v}}(y,w) = \frac{1}{\sqrt{8\,\pi}}\,\frac{m_x^{m_x}\,m_y^{m_y}\,y^{m_y-\frac{3}{2}}}{\Gamma\left(m_x\right)\,\Gamma\left(m_y\right)}\int\limits_0^{\infty}\frac{x^{m_x-m_y-\frac{1}{2}}}{\sqrt{b_x^2\,y+b_y^2\,x^2}} \times \exp\left[-m_x\,x-\frac{m_y\,y}{x}-\frac{w^2\,x}{8\,y\,(b_x^2\,y+b_y^2\,x^2)}\right]dx\,, \tag{14}$$

where v corresponds to the normalized power

$$v = \frac{z}{\overline{P}_{\rm in}}\,, \tag{15}$$

and parameters b_x and b_y are the standard deviations of the time derivative of the random processes associated with the large scale and small scale scattering [9]. The calculation of the LCR for a specific BER level, however, requires the derivation of the joint pdf between the BER rv b and its time derivative. To this end, we utilize (8) to associate b with v as

$$b = BER\left(v\,\overline{P}_{\rm in}\right) \Rightarrow v = \frac{T\left(b\right)}{\overline{P}_{\rm in}}\,, \tag{16}$$

where $T\left(\cdot\right)$ denotes the inverse BER function. The joint pdf for the BER is calculated by changing variables as

$$v = \frac{T\left(b\right)}{\overline{P}_{\rm in}}\,, \tag{17a}$$

$$\dot{v} = \frac{T'\left(b\right)}{\overline{P}_{\rm in}}\,\dot{b} \tag{17b}$$

and after combining (14) and (17) we find that

$$f_{b,\dot{b}}\left(y,w\right) = \left(\frac{T'\left(y\right)}{\overline{P}_{\rm in}}\right)^2 f_{v,\dot{v}}\left(\frac{T\left(y\right)}{\overline{P}_{\rm in}}, w\,\frac{T'\left(y\right)}{\overline{P}_{\rm in}}\right)\,. \tag{18}$$

From its definition, the LCR is finally calculated by

$$\begin{aligned} LCR\left(P_{\rm s}\right) &= \int_0^{\infty} f_{b,\dot{b}}\left(BER_0,\,w\right)\,w\,dw = \left(\frac{T'\left(BER_0\right)}{\overline{P}_{\rm in}}\right)^2 \\ &\times \int_0^{\infty} f_{v,\dot{v}}\left(\frac{T\left(BER_0\right)}{\overline{P}_{\rm in}}, w\,\frac{T'\left(BER_0\right)}{\overline{P}_{\rm in}}\right)\,w\,dw \\ &= \int_0^{\infty} f_{v,\dot{v}}\left(\frac{P_{\rm s}}{\overline{P}_{\rm in}}, q\right)\,q\,dq\,, \end{aligned} \tag{19}$$

where $P_{\rm s}$ is the receiver sensitivity that achieves the required BER level. Clearly, (19) is equal to the LCR that is calculated for the $\gamma-\gamma$ channel at the receiver sensitivity.

The LCR of the SOA-assisted system is plotted in Figs. 3 and 4 against the average input power for target BERs of

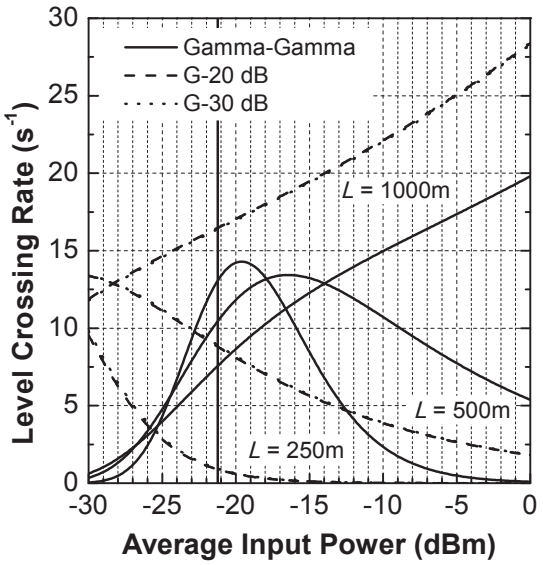

Fig. 3. Average level crossing rates versus the average input power for $BER_0 = 10^{-3}$. The solid vertical line corresponds to the receiver sensitivity without SOA.

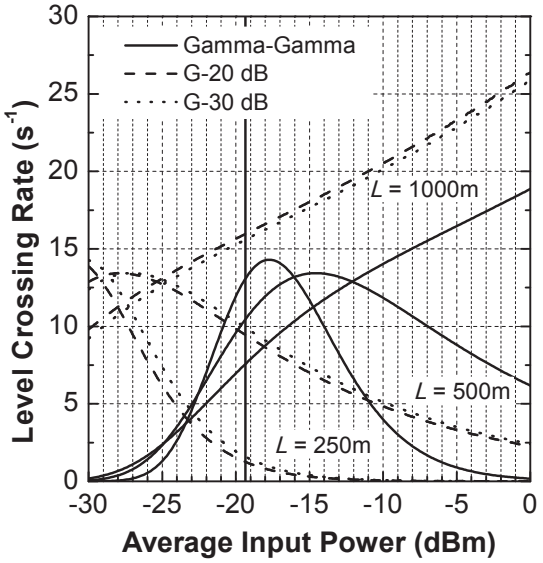

Fig. 4. Average level crossing rates versus the average input power for $BER_0 = 10^{-6}$. The solid vertical line corresponds to the receiver sensitivity without SOA.

10^{-3} and 10^{-6}. The results show that the LCR is modified by the power margin that is provided by the sensitivity increase from the SOA. For the 250 and 500 m link and average powers beyond the original system sensitivity the LCR is decreased by a significant factor, which implies that the SOA may worsen the AFD performance of the system according to (20). In contrast, the SOA increases the LCR of 1000 m link irrespective of the power level. As a result, it is not possible to draw a definitive conclusion for the SOA-assisted system performance from the LCR alone and an AFD analysis is required.

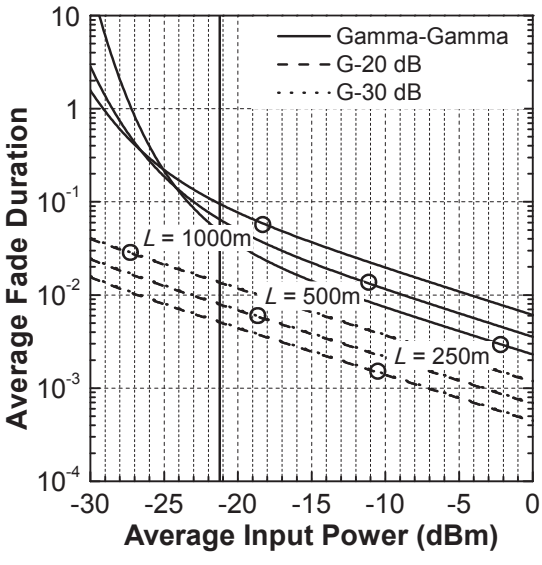

Fig. 5. Average fade duration versus average input power for $BER_0 = 10^{-3}$. The solid vertical line corresponds to the receiver sensitivity without SOA.

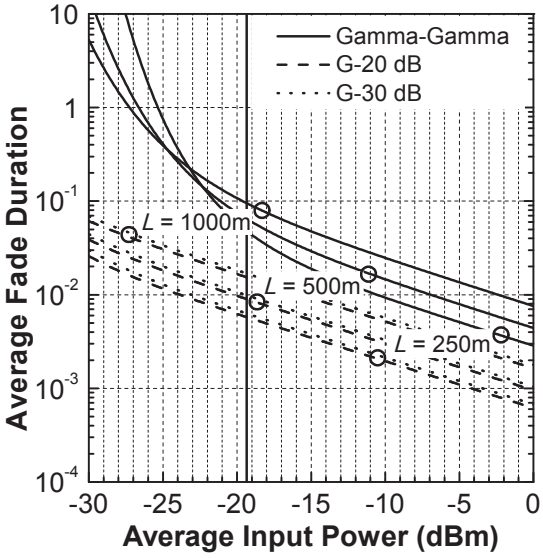

Fig. 6. Average fade duration versus average input power for $BER_0 = 10^{-6}$. The solid vertical line corresponds to the receiver sensitivity without SOA.

The AFD is given by

$$AFD\left(P_{\mathrm{s}}\right) = \frac{\Pr\left\{z \leq P_{\mathrm{s}}\right\}}{LCR\left(P_{\mathrm{s}}\right)} \tag{20}$$

and can be directly calculated from (19) and

$$\Pr\left\{z \leq P_{\mathrm{s}}\right\} = \int_{0}^{P_{\mathrm{s}}} f_{P_{\mathrm{in}}}(z)\, dz\,, \tag{21}$$

with the aid of (1).

Numerical results for AFD are plotted against the average input power in Figs. 5 and 6 for BER targets if 10^{-3} and 10^{-6}, respectively, similarly to the previous analysis. The results illustrate that, in contrast with the LCR, the SOA always

improves the AFD performance of the system irrespective of the input power. In fact, the AFD in the SOA-assisted system is reduced by more than 80% of its original value for the 10^{-3} BER target and by more than 76% for the 10^{-6} target. Clearly, this corresponds to a very drastic improvement on the AFD.

V. Conclusions and Future Work

We have presented novel analytical results for a SOA amplified OWC system and have demonstrated that the sensitivity improvement that is achieved by optical amplification also improves the system performance as measured by key first and second-order metrics. With respect to first-order statistics, the SOA-assisted system exhibits significantly lower average BERs and higher link availabilities. In a similar fashion, the sensitivity improvement can be utilized to partially or fully compensate for the fade margin in medium-to-strong turbulence for link lengths that do not exceed several hundreds of meters. As far as the second-order statistics are concerned, we have presented analytical results on the amplified system LCR and AFD for the first time to our knowledge. The results clearly demonstrate a drastic improvement of the AFD irrespective of the link length. In addition, we have showed that the LCR and AFD can be calculated from the sensitivity of the amplified system alone, and this is of practical importance for future works that will extend the scope of LCR and AFD study to the weak and saturated turbulence regimes. In both regimes, a similar analysis can be readily performed provided that the outage probability and LCR is known for log-normal and exponential statistics, respectively.

Acknowledgment

This work was funded by the University of Peloponnese internal project FAMOOSE and supported by COST Action IC1101 "Optical Wireless Communications–An Emerging Technology".

References

[1] V. W. S. Chan, "Optical satellite networks," *J. Lightw. Technol.*, vol. 21, no. 11, pp. 2811–2827, Nov. 2003.

[2] Z. Sodnik, B. Furch, and H. Lutz, "Optical intersatellite communication," *IEEE J. Sel. Topics Quantum Electron.*, vol. 16, no. 5, pp. 1051–1057, Sep. 2010.

[3] D. M. Boroson, J. J. Scozzafava, D. V. Murphy, B. S. Robinson, and H. Shaw, "The lunar laser communications demonstration (llcd)," in *Proc. 3rd IEEE Intern. Conf. Space Mission Challenges Inform. Technol. (SMC-IT 2009)*, Jul. 2009, pp. 23–28.

[4] D. Kedar and S. Arnon, "Urban optical wireless communication networks: The main challenges and possible solutions," *IEEE Commun. Mag.*, vol. 42, no. 5, pp. S2–S7, May 2004.

[5] R. S. Lawrence and J. W. Strohbehn, "A survey of clear-air propagation effects relevant to optical communications," in *Proc. IEEE*, vol. 58, no. 10, Oct. 1970, pp. 1523–1545.

[6] M. Ijaz, Z. Ghassemlooy, J. Pesek, O. Fiser, H. L. Minh, and E. Bentley, "Modeling of fog and smoke attenuation in free space optical communications link under controlled laboratory conditions," *J. Lightw. Technol.*, vol. 31, no. 11, pp. 1720–1726, Jun. 2013.

[7] M. Hulea, Z. Ghassemlooy, S. Rajbhandari, and X. Tang, "Compensating for optical beam scattering and wandering in FSO communications," *J. Lightw. Technol.*, vol. 32, no. 7, pp. 1323–1328, Apr. 2014.

[8] H. Yuksel, S. Milner, and C. C. Davis, "Aperture averaging for optimizing receiver design and system performance on free-space optical communication links," *OSA J. Opt. Netw.*, vol. 4, no. 8, pp. 462–475, Jul. 2005.

[9] F. S. Vetelino, C. Young, L. Andrews, and J. Recolons, "Aperture averaging effects on the probability density of irradiance fluctuations in moderate-to-strong turbulence," *Appl. Opt.*, vol. 46, no. 11, pp. 2099–2108, Apr. 2007. [Online]. Available: http://ao.osa.org/abstract.cfm?URI=ao-46-11-2099

[10] M.-A. Khalighi, N. Schwartz, N. Aitamer, and S. Bourennane, "Fading reduction by aperture averaging and spatial diversity in optical wireless systems," *IEEE/OSA J. Opt. Netw.*, vol. 1, no. 6, pp. 580–593, Nov. 2009.

[11] W. O. Popoola and Z. Ghassemlooy, "BPSK subcarrier intensity modulated free-space optical communications in atmospheric turbulence," *J. Lightw. Technol.*, vol. 27, no. 8, pp. 967–973, Apr. 2009.

[12] M. Niu, J. Cheng, and J. F. Holzman, "MIMO architecture for coherent optical wireless communication: System design and performance," *IEEE/OSA J. Optical Commun. Netw.*, vol. 5, no. 5, pp. 411–420, May 2013.

[13] A. Anguita, M. A. Neifeld, B. Hildner, and B. Vasic, "Rateless coding on experimental temporally correlated FSO channels," *J. Lightw. Technol.*, vol. 28, no. 7, pp. 990–1002, Apr. 2010.

[14] M. Uysal, J. Li, and M. Yu, "Error rate performance analysis of coded free-space optical links over gamma-gamma atmospheric turbulence channels," *IEEE Trans. Wireless Commun.*, vol. 5, no. 6, pp. 1229–1233, Jun. 2006.

[15] C. K. Datsikas, K. P. Peppas, N. C. Sagias, and G. S. Tombras, "Serial free-space optical relaying communications over gamma-gamma atmospheric turbulence channels," *IEEE/OSA J. Optical Commun. Netw.*, vol. 2, no. 8, pp. 576–586, Aug. 2010.

[16] E. Bayaki, D. S. Michalopoulos, and R. Schober, "EDFA-based all-optical relaying in free-space optical systems," *IEEE Trans. Commun.*, vol. 60, no. 12, pp. 3797–3807, Dec. 2012.

[17] S. Kazemlou, S. Hranilovic, and S. Kumar, "All-optical multihop free-space optical communication systems," *Lightwave Technology, Journal of*, vol. 29, no. 18, pp. 2663–2669, Sept 2011.

[18] M. Kashani, M. Rad, M. Safari, and M. Uysal, "All-optical amplify-and-forward relaying system for atmospheric channels," *Communications Letters, IEEE*, vol. 16, no. 10, pp. 1684–1687, October 2012.

[19] M. Abtahi, P. Lemieux, W. Mathlouthi, and L. A. Rusch, "Suppression of turbulence-induced scintillation in free-space optical communication systems using saturated optical amplifiers," *J. Lightw. Technol.*, vol. 24, no. 12, pp. 4966–4973, Dec. 2006.

[20] K. Yiannopoulos, N. C. Sagias, and A. C. Boucouvalas, "Fade mitigation based on semiconductor optical amplifiers," *J. Lightw. Technol.*, vol. 31, no. 23, pp. 3621–3630, Dec. 2013.

[21] N. A. Olsson, "Lightwave systems with optical amplifiers," *J. Lightw. Technol.*, vol. 7, no. 7, pp. 1071–1082, Jul. 1989.

[22] P. A. Humblet and M. Azizoglu, "On the bit error rate of lightwave systems with optical amplifiers," *J. Lightw. Technol.*, vol. 9, no. 11, pp. 1576–1582, Nov. 1991.

[23] M. Razavi and J. H. Shapiro, "Wireless optical communications via diversity reception and optical preamplification," *IEEE Trans. Wireless Commun.*, vol. 4, no. 3, pp. 975–983, May 2005.

[24] K. Yiannopoulos, N. C. Sagias, and A. C. Boucouvalas, "On the performance of semiconductor optical amplifier-assisted outdoor optical wireless links," *IEEE J. Sel. Areas Commun.*, May 2014, submitted.

[25] P. S. Bithas, N. C. Sagias, P. T. Mathiopoulos, G. K. Karagiannidis, and A. A. Rontogiannis, "On the performance analysis of digital communications over generalized-K fading channels," *IEEE Commun. Lett.*, vol. 10, no. 5, pp. 353–355, May 2006.

[26] M. Eiselt, W. Pieper, and H. G. Weber, "SLALOM: Semiconductor laser amplifier in a loop mirror," *J. Lightw. Technol.*, vol. 19, no. 10, pp. 2099–2112, Oct. 1995.

[27] G. P. Agrawal, *Fiber-Optic Communication Systems*, ser. Wiley Series in Microwave and Optical Engineering. Wiley, 2012. [Online]. Available: http://books.google.gr/books?id=yGQ4n1-r2eQC

[28] F. S. Vetelino, "Fade statistics for a lasercom system and the joint pdf of a gamma-gamma distributed irradiance and its time derivative," Doctoral dissertation, University of Central Florida, Florida, USA, Jan. 2006.